Identification and characterization of a negative regulator of FtsZ ring formation in *Bacillus subtilis*

Petra Anne Levin, Iren G. Kurtser, and Alan D. Grossman*

Department of Biology, Building 68-530, Massachusetts Institute of Technology, Cambridge, MA 02139

ABSTRACT During the bacterial cell cycle, the tubulin-like cell-division protein FtsZ polymerizes into a ring structure that establishes the location of the nascent division site. We have identified a regulator of FtsZ ring formation in *Bacillus subtilis*. This protein, EzrA, modulates the frequency and position of FtsZ ring formation. The loss of *ezrA* resulted in cells with multiple FtsZ rings located at polar as well as medial sites. Moreover, the critical concentration of FtsZ required for ring formation was lower in *ezrA* null mutants than in wild-type cells. EzrA was associated with the cell membrane and also colocalized with FtsZ to the nascent septal site. We propose that EzrA interacts either with FtsZ or with one of its binding partners to promote depolymerization.

Cytokinesis in nearly all bacteria begins with polymerization of the essential GTPase FtsZ into a ring structure at the nascent division site (1). FtsZ initially localizes to division sites as small foci, which then extend bidirectionally around the circumference of the cells to form complete rings (1). The FtsZ ring is required for recruitment of other cell-division proteins and serves as a framework for assembly of other components of the division machinery (1–3). Two questions frame current research on FtsZ: (*i*) what regulates the transition between FtsZ monomer and polymer during the cell cycle? and (*ii*) what factors govern FtsZ localization?

FtsZ is subject to temporal, spatial, and developmental regulation in the Gram-positive bacterium *Bacillus subtilis*. During exponential growth, FtsZ rings form exclusively at midcell as a prelude to binary fission. In contrast, at the onset of sporulation (a developmental pathway initiated in response to nutrient deprivation and cell crowding), FtsZ shifts from a medial to a bipolar pattern of localization, forming a ring near each pole of the cell (4). Despite the presence of two FtsZ rings, only one polar site is used for cell division, indicating that FtsZ ring formation is not sufficient to drive septation.

Several regulators of FtsZ have been identified (1). One, the product of the *Escherichia coli sulA* gene, is induced after DNA damage as part of the SOS response. SulA binds to and inhibits the GTPase activity of FtsZ, preventing polymerization (5, 6). Another *E. coli* protein, ZipA, binds FtsZ directly (7) and is involved in stabilizing the FtsZ ring during cytokinesis (8). In *B. subtilis* and *E. coli*, the products of *minC* and *minD* function in tandem to prevent polar septation (9). Mutations in *minC* and *minD* result in the formation of polar FtsZ rings and anucleate minicells (9, 10). MinD localizes to the cell poles in *B. subtilis* (11) and in *E. coli*, where it shifts between the two poles in a periodic manner (12).

Control of FtsZ ring formation may be analogous to the control of tubulin polymerization in eukaryotes. The crystal structures of FtsZ and the α/β tubulin dimer indicate that the folded proteins closely resemble one another, even in regions of limited sequence similarity (13–15). In addition, FtsZ polymerizes in a GTP-dependent manner, forming protofilaments, sheets, and minirings *in vitro* akin to those formed by tubulin under similar conditions (16). Despite these similarities, and with the possible exception of ZipA (8), homologues of proteins known to regulate tubulin polymerization have not been found in *B. subtilis* or other eubacteria.

We have identified a gene, *ezrA*, whose product is an inhibitor of FtsZ ring formation. The loss of *ezrA* allows cells carrying a temperature-sensitive allele of *ftsZ* to form FtsZ rings at high temperatures. In *ftsZ*$^+$ cells, an *ezrA* null mutation causes the formation of multiple FtsZ rings. Moreover, the concentration of FtsZ required for ring formation is significantly lower in *ezrA* null mutants than in wild-type cells. EzrA colocalizes with FtsZ at the nascent division site, suggesting that it interacts with FtsZ or with other components of the division machinery.

MATERIALS AND METHODS

General Methods. Standard techniques were used for cloning and for genetic manipulation (17, 18). *B. subtilis* strains are derivatives of JH642 (19) and contain the *trpC2* and *pheA1* mutations. Cells were grown in rich [LB (18)] or minimal [S7$_{50}$ 1% glucose/0.1% glutamate (20)] medium supplemented with appropriate amino acids at 37°C unless otherwise noted. Sporulation was induced by resuspension in sporulation salts or by exhaustion in Difco sporulation medium (17).

Strains and Plasmids. Plasmids for creating *ftsZ-gfp, ezrA-gfp,* and *ezrA-myc* were built by fusing a 3' fragment of either *ftsZ* or *ezrA* to the 5' end of either *gfp* or *myc*. The *myc* tag was derived from the *Saccharomyces cerevisiae* vector pRH177/23 (21) and the *gfp* tag from the *B. subtilis* vector pDL50B (22). The blue fluorescent protein (BFP) fusion was constructed by site-directed mutagenesis of an *ezrA-gfpmut2* fusion (23) to make the Y66H mutation, resulting in a blue variant of green fluorescent protein (GFP) (24) (QuikChange Kit, Stratagene). Full length carboxyl-terminal fusions to GFP, BFP, or Myc were constructed by single crossover integration of the appropriate plasmid directly into the chromosomal locus. The P$_{spac}$-*ftsZ-gfp* fusion at the *amyE* locus encodes the *ftsZ-gfp* fusion amplified from PL642 chromosomal DNA and cloned under the control of the LacI-repressible isopropyl-D-thiogalactoside (IPTG)-inducible promoter P$_{spac}$ in the vector pDR67 (25). The *ezrA* null allele is an insertion of a *spc* cassette (spectinomycin resistance) between codons 145 and 146.

Isolation and Mapping of Suppressor Mutations. Within 14 hr of plating the *ftsZ-gfp* strain PL642 onto selective medium (LB chloramphenicol 5 μg/ml) at 45°C, two classes of temperature-resistant colonies were visible, large and small. Both large and small temperature-resistant colonies were obtained at a frequency of 10^{-5} to 10^{-6}. The small colonies did not maintain their temperature-resistant phenotype after passage

at permissive temperature (30°C). In contrast, the large colonies maintained temperature resistance after multiple passages at 30°C. Transformation of DNA from the suppressor-bearing strains into wild-type cells confirmed that the suppressor mutations in the large colonies were not linked to the *ftsZ-gfp* allele. Three independent isolates were chosen for further characterization. The linkage of the *ezrA* mutations to known chromosomal markers was determined by using PBS1-mediated transduction and DNA-mediated transformation (17). Secondary structure analysis of the *ezrA* gene product was performed by using the TMPREDICT and COILS programs (26, 27).

Fluorescence Microscopy. Live cells were sampled directly onto microscope slides. Strains encoding GFP fusions were grown at 30°C. Cells were prepared for immunofluorescence microscopy either by paraformaldehyde-gluteraldehyde fixation (28, 29) or by a modified methanol fixation (ref. 30; E. A. Angert, personal communication). Wheat germ agglutinin (lectin) conjugated to the green fluorophore FITC (Molecular Probes) was used to visualize cell walls (31).

Some images were recorded on 35-mm slide film (Kodak EliteII) and then digitized by using a Nikon Coolscan II slide scanner. Others were captured digitally by using either a color charge-coupled device (CCD) camera (Optronics Engineering) and SCION IMAGE software or a black and white ORCA CCD camera (Hammamatsu, Middlesex, NJ) and OPENLABS 1.7.8 software. GFP and BFP were visualized by using Chroma (Brattleboro, VT) filter sets no. 41012 and no. 31000, respectively. Images were processed by using ADOBE PHOTOSHOP 3.0 (Adobe Systems, Mountain View, CA).

Affinity purified IgG and IgY antibodies against FtsZ were described previously (4, 22). Polyclonal antibodies against GFP (CLONTECH) were used at a 1:4,000 dilution. Monoclonal antibodies against the Myc epitope (Zymed) were used at a 1:10,000 dilution. Secondary antibodies coupled to FITC or Cy-3 were from Jackson ImmunoResearch.

RESULTS

Isolation of Extragenic Suppressors of a Temperature-Sensitive Allele of *ftsZ*. We have noticed that fusing proteins to the GFP occasionally renders them temperature sensitive for function. This defect is most likely caused by misfolding of the GFP moiety and potentially the entire fusion protein at higher temperatures (32). In contrast to *E. coli* (33), *B. subtilis* cells in which the only copy of *ftsZ* is fused to *gfp* (PL642) are viable at 30°C but unable to form colonies at ≥45°C.

The FtsZ–GFP fusion was defective in its ability to form new FtsZ rings at the restrictive temperature. At the permissive temperature, most PL642 cells had rings of FtsZ-GFP, as measured by immunofluorescence microscopy (Fig. 1*A*). In contrast, after a shift to 45°C, the number of cells with rings of FtsZ-GFP steadily decreased. After 45 min at 45°C, very few rings of FtsZ-GFP were visible (Fig. 1*B*). Raising the intracellular concentration of FtsZ-GFP by placing an additional copy of *ftsZ-gfp* at a second locus partially suppressed the temperature sensitivity of the fusion.

Starting with the temperature-sensitive *ftsZ-gfp* strain (PL642), we isolated extragenic suppressors that restored viability at 45°C (*Materials and Methods*). FtsZ rings were visible in immunofluorescence micrographs of one of the temperature-resistant isolates (PL710) at 30°C and after 45 min of growth at 45°C (Fig. 1 *C* and *D*). This contrasts markedly with the single FtsZ ring observed in a field of cells from the parent strain cultured under identical conditions (Fig. 1*B*). Three independent suppressor mutations, all of which were subsequently mapped to the same locus, were chosen for further characterization. None of the mutations suppressed the temperature sensitivity of a strain carrying a *gfp* fusion to a gene (*dnaI*) required for DNA replication (data not shown).
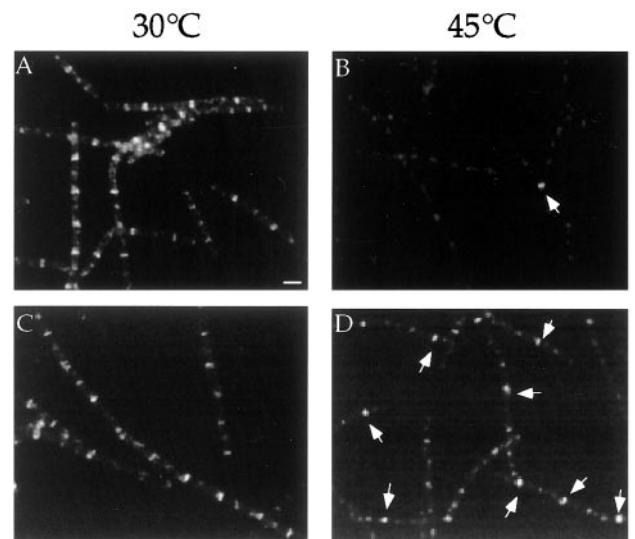

FIG. 1. Localization of FtsZ-GFP. Cells containing *ftsZ-gfp* were grown in LB to exponential phase (OD600 ≈ 0.5) at 30°C, then diluted 1:5 into fresh medium at 30°C (*A* and *C*) or 45°C (*B* and *D*). Samples were taken 45 min after dilution and analyzed by immunofluorescence microscopy by using primary antibodies against FtsZ and a Cy-3-conjugated secondary antibody. FtsZ rings appear as bands across the short axis of the cell. (*A* and *B*) PL642 (*ftsZ-gfp*) at 30°C (*A*) and after 45 min of growth at 45°C (*B*). Note that only a single ring of FtsZ is visible in this field of cells (arrow). (*C* and *D*) PL710 (*ftsZ-gfp ezrA1*) at 30°C (*C*) and after 45 min of growth at 45°C (*D*). Arrows indicate representative FtsZ rings. Bars = 1 μm.

The suppressor mutations caused the formation of multiple FtsZ rings in *ftsZ*⁺ strains as expected. Immunofluorescence microscopy indicated that wild-type cells had single medially positioned FtsZ rings (Fig. 2 *A* and *B*), as described previously (4). In contrast, multiple rings of FtsZ were detected at polar and medial positions in the majority of *ftsZ*⁺ cells carrying the suppressor mutations (Fig. 2 *C* and *D*). We designated the mutations *ezrA*, for extra Z rings A.

The *ezrA* Alleles Map to a Single ORF. The three *ezrA* mutations were in the 562-codon ORF previously designated *ytwP* by the *B. subtilis* genome project (34). Two of the *ezrA* alleles encoded nonsense mutations that truncate the putative *ezrA* gene product by 178 and 166 aa, respectively. The third *ezrA* mutation was not sequenced. *ezrA* appears to be monocistronic because the upstream (*ytvP*) and downstream (*braB*) genes are transcribed in the opposite direction from *ezrA*.

The *ezrA* gene product is predicted to be ≈65 kDa with a 19-residue membrane-spanning domain in the amino-terminal region and four coiled-coil motifs distributed along its length. EzrA is strongly predicted to be oriented with its carboxyl-terminal domain in the cytoplasm. EzrA is conserved in several Gram-positive bacteria but has not been found in any Gram-negative bacteria whose sequences are available (http://www.ncbi.nlm.nih.gov/BLAST/unfinishedgenome.html). An *ezrA* null mutation (an insertion in the 5′ end), like the original *ezrA* mutations, suppressed the temperature-sensitive phenotype of the *ftsZ-gfp* allele. Furthermore, in an *ftsZ*⁺ background, the *ezrA* null allele increased the frequency and altered the position of FtsZ ring formation (Fig. 2 *E* and *F*; also, see below).

Increased Frequency of FtsZ Ring Formation in the *ezrA* Null Mutant. We analyzed the frequency and position of FtsZ ring formation in wild-type and *ezrA* null mutant cells under various growth conditions. In confirmation of our previous results, over 95% of wild-type cells have single medial rings of FtsZ during rapid growth in rich medium (LB) (Fig. 2 *A* and *B*; Fig. 3*A*), whereas only ≈60% have FtsZ rings during slower

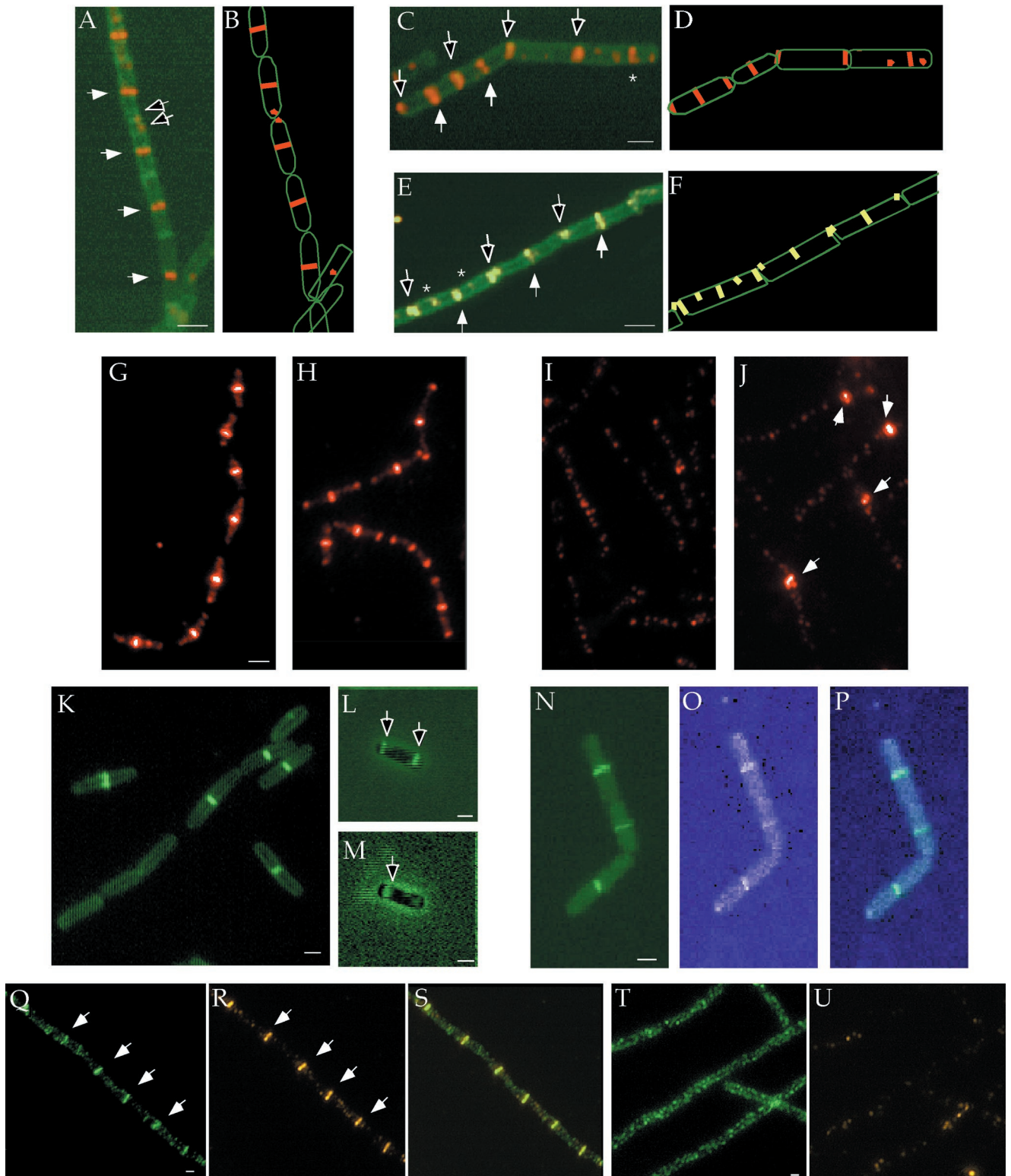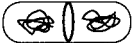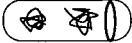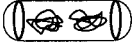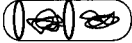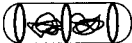FIG. 2.   Localization of FtsZ and EzrA. (*A–F*) Localization of FtsZ in wild-type and *ezrA* mutant cells during exponential growth in LB at 37°C. (*A, C,* and *E*). FtsZ is stained red or yellow (because of the use of different filter sets) and the cell wall is stained green (see *Materials and Methods.*) Closed arrows indicate medial FtsZ rings. Open arrows point to polar rings or foci of FtsZ. Asterisks denote rings or foci of FtsZ at quarter positions. Merged images of FtsZ and cell walls (*A, C,* and *E*) and cartoons of the micrographs (*B, D,* and *F*). (*A* and *B*) Wild-type cells. Note the even spacing of the medially positioned FtsZ rings. Small foci of FtsZ are occasionally visible at the cell poles (open arrows). (*C* and *D*) *ezrA1 ftsZ*⁺ cells (PL730). The irregular spacing of the FtsZ rings in the *ezrA*⁻ cells is because of FtsZ localization at polar and medial positions. Some cells have multiple FtsZ rings. The cell on the upper right has a single FtsZ ring at a quarter position. (*E* and *F*) *ezrA::spc, ftsZ*⁺ cells (PL867). (*G–J*) Localization of FtsZ in *ezrA*⁺ (*G* and *I*) and *ezrA* mutant cells (*H* and *J*) before (*G* and *H*) and 100 min after (*I* and *J*) depletion of FtsZ. Strains PL919 (*ezrA*⁺ P_spac−ftsZ) and PL928 (*ezrA::spc* P_spac−ftsZ) were grown in LB at 37°C in the presence of IPTG (1 mM to express *ftsZ*) and chloramphenicol (2 μg/ml to maintain the Pspac-ftsZ plasmid). At mid- to late exponential phase, cells were washed and diluted 1:10 in LB with chloramphenicol with (*G* and *H*) and without IPTG (*I* and *J*). FtsZ is immunostained red. The exposure times in *G* and *H* and in *I* and *J* are identical. Arrows point to rings of FtsZ in the *ezrA* mutant cells after FtsZ depletion. (*K–M*) Localization of EzrA-GFP in live cells, strain PL847, grown at 30°C. (*K*) EzrA-GFP

A

	wild type	*ezrA⁻*
	>99% (164)	32% (91)
	<1% (0)	9.9% (28)
	<1% (0)	5.3% (15)
	<1% (0)	27% (77)
	<1% (0)	9.9% (28)
Others	<1% (0)	16% (44)
Total	164	283
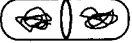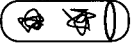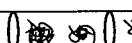
B

	wild type	*ezrA⁻*
	>99% (148)	91% (380)
	<1% (1)	4.1% (17)
	<1% (0)	2.4% (10)
	<1% (0)	2.4% (10)
Total	149	417

FIG. 3. ezrA mutant cells have extra rings of FtsZ. Wild-type (JH642) and *ezrA* null mutant cells (PL867) were grown in rich LB (*A*) or defined minimal medium (*B*). Samples were taken during exponential growth and the number and position of FtsZ rings was analyzed by immunofluorescence microscopy. Only cells with visible FtsZ rings were counted and the total number of cells in each class is indicated in parentheses. "Others" represents the classes of cells that had four or more FtsZ rings. In general, these cells were longer than cells with fewer FtsZ rings. Data on wild-type cells in LB were previously published (10). In minimal medium, cells with FtsZ rings at the quarter positions were generally longer than cells in the other two classes.

growth in minimal medium (4, 10, 22). The remainder of wild-type cells had no apparent FtsZ rings.

In contrast, 54% (164/300) of *ezrA* null mutant cells had more than one FtsZ ring located at polar and/or medial positions (Fig. 2 *E* and *F*; Fig. 3*A*). Of the *ezrA* mutant cells with single FtsZ rings, 76% (91/119) had a medial and 24% (28/119) had a polar FtsZ ring. The bias toward medial FtsZ localization implies that midcell is still the favored site for FtsZ ring formation in the *ezrA* mutant.

The percentage of *ezrA* null mutant cells with multiple FtsZ rings decreased dramatically under slower growth conditions. Of the *ezrA* mutant cells with FtsZ rings, 98% (407/417) had

only one FtsZ ring after growth in minimal medium (doubling time ≈45 min) (Fig. 3*B*). Cells with polar FtsZ rings accounted for only 4% (17/417) of the population of *ezrA* null cells with rings. The cells with more than one FtsZ ring (10/417) were longer, and the extra FtsZ rings were generally located at quarter positions (Fig. 3*B*). These results are similar to our previous observation regarding the frequency of FtsZ ring formation in *minCD* null mutants (10). In rich medium, *minCD* null mutant cells often have multiple rings of FtsZ, whereas in minimal medium the overwhelming majority of cells have only a single FtsZ ring (10). Together, these results indicate the presence of a growth-dependent mechanism that regulates the frequency of FtsZ ring formation.

Although the loss of *ezrA* changed the frequency of FtsZ ring formation in individual cells, it did not significantly alter the proportion of cells that had FtsZ rings. In rich medium, ≈97% of wild-type cells (164/169) and ≈94% (283/300) of *ezrA* mutant cells had FtsZ rings. Likewise, in minimal medium FtsZ rings were found in ≈58% (199/344) of wild-type cells and ≈66% (169/257) of the *ezrA* mutant cells. These results suggest that EzrA does not influence the cell-cycle signal initiating FtsZ polymerization but rather functions subsequently to inhibit FtsZ ring formation at polar sites.

FtsZ localization was not random in the *ezrA* mutants. FtsZ rings were observed only at positions that could be described as past, present, or future division sites. A small fraction of cells had FtsZ rings or FtsZ foci at the cell quarters (Fig. 2 *E* and *F*, lower left cell). These are most likely cells that failed to divide in the previous generation. Despite its limited effect on the number of cells with an FtsZ ring, an *ezrA* null mutation appeared to cause a delay in division. Although their mass doubling times were virtually identical, *ezrA* null mutants were ≈20% longer on average than their wild-type counterparts during growth in minimal medium.

Cell Division and Sporulation in the *ezrA* Null Mutant. Formation of polar FtsZ rings can lead to polar divisions and the formation of anucleate minicells (35). Although ≈50% of all the FtsZ rings were polar in the *ezrA* null mutant grown in rich medium, minicells constituted only 3.7% (42/1151) of the cells. Thus, only a small percentage of the polar FtsZ rings were used for division. A similar situation is also observed in *B. subtilis* cells at the onset of sporulation in which only one of two polar rings is used for septation (4) and in *B. subtilis minCD* null mutants during vegetative growth in rich medium (10), indicating that the presence of an FtsZ ring is not sufficient for septation. The *ezrA* null mutation did not significantly alter the sporulation efficiency of an otherwise wild-type strain.

Loss of *minCD* Does Not Suppress *ftsZ-gfp*. Mutations in *B. subtilis minC* and *minD* result in the formation of multiple rings of FtsZ in rapidly growing cells, a phenotype similar to that of the *ezrA* null mutant (10). However, it appears that MinCD and EzrA have different modes of action, and therefore effect different aspects of FtsZ ring formation. Significantly, a *minCD* null mutation did not suppress the temperature-sensitive phenotype caused by *ftsZ-gfp*, indicating that the loss of MinCD is not sufficient to overcome the defect in FtsZ-GFP. Moreover, the polar FtsZ rings are used more frequently

in vegetatively growing cells sampled from solid rich medium. EzrA-GFP is distributed throughout the membrane and appears in some cells as a band or ring at midcell. (*L* and *M*) Localization of EzrA-GFP in cells 1.5 (*L*) and 3 (*M*) hr after the initiation of sporulation. Fluorescence and phase contrast images are superimposed. Open arrows point to polar rings of EzrA. (*N–P*) Colocalization of FtsZ-GFP and EzrA-BFP in live cells. Strain PL995 (*ezrA-bfp ftsZ⁺ P꜀ₚₐ꜀-ftsZ-gfp*) was grown in LB at 30°C (5 μM IPTG) and sampled during exponential growth. (*N*) FtsZ-GFP. (*O*) EzrA-BFP. (*P*) Overlay of FtsZ-GFP (*N*) and EzrA-BFP (*O*). (*Q–U*) Localization of EzrA-GFP in the presence and absence of FtsZ. FtsZ depletion was carried out essentially as described above. Strain PL851 (*ezrA-gfp P꜀ₚₐ꜀-ftsZ*) was grown in LB at 30°C in the presence (*Q–S*) or absence of IPTG (*T* and *U*). Samples were taken after approximately four mass doublings, fixed, and prepared for immunofluorescence microscopy. EzrA-GFP is immunostained green and FtsZ is immunostained red. (*Q*) EzrA-GFP. (*R*) FtsZ. (*S*) overlay of EzrA-GFP (*Q*) and FtsZ (*R*). (*T*) EzrA-GFP without IPTG, after depletion of FtsZ. Rings are no longer visible in these cells. Instead, only a punctate pattern of bright fluorescence is observed. (*U*) Residual FtsZ staining after depletion. The exposure time is the same as that in *T*. Very little FtsZ protein is present and ring formation is abolished. Bars = 1 μm.

for cell division in the *minCD* null mutant cells (10) than they were in the absence of *ezrA*; in rich medium, the frequency of minicell formation is four times higher in a *minCD* null mutant than it was in a congenic *ezrA* null mutant strain. This observation may indicate that the MinCD complex is involved in preventing existing FtsZ rings from maturing. Finally, EzrA and MinD are found in different subcellular locations (see below).

The Critical Concentration of FtsZ Required for Ring Formation Is Lower in *ezrA* Mutant Cells. The effects of the *ezrA* null mutations on FtsZ ring formation were not caused by changes in FtsZ protein levels. Two to seven-fold overexpression of *ftsZ* in *E. coli* leads to polar divisions and the formation of anucleate minicells, suggesting that increased levels of FtsZ result in polar ring formation (36). In *B. subtilis,* we found that increasing *ftsZ* levels 2-fold or greater leads to the formation of polar FtsZ rings (P.A.L., unpublished data). However, quantitative immunoblotting indicated that the amount of FtsZ was similar in wild-type and *ezrA* mutant cells (data not shown).

Because the loss of EzrA resulted in a phenotype similar to that observed in cells with increased levels of FtsZ, we postulated that EzrA effects the critical concentration of FtsZ required to initiate ring formation. We examined the frequency of cells with FtsZ rings after depletion of FtsZ in a strain (PL919) carrying a copy of *ftsZ* under the control of the LacI-repressible IPTG-inducible promoter P$_{spac}$ and a congenic *ezrA* null mutant (PL928). In the presence of IPTG, the *ezrA*$^+$ cells had single medially positioned FtsZ rings, whereas the *ezrA* null mutants displayed the aberrant pattern of polar and medial FtsZ ring formation described above (Fig. 2 *G* and *H*). However, 100 min after growth in the absence of IPTG, only 7.6% of wild-type cells (13/170) had an FtsZ ring (Fig. 2*I*). By comparison, at the same time point over 60% (112/179) of the *ezrA* null mutant cells had FtsZ rings (Fig. 2*J*).

De novo FtsZ ring formation occurred at a lower FtsZ concentration in the *ezrA* mutant than in wild-type cells. After 120 min of growth in the absence of IPTG, <1% of wild-type and *ezrA* mutant cells had FtsZ rings. At this time point, we added IPTG and found that after 10 min both strains had FtsZ rings spaced along the cell filaments, as visualized by immunofluorescence microscopy. However, the frequency of FtsZ ring formation relative to cell length was approximately 2-fold higher in the *ezrA* null mutant, indicating that more FtsZ rings were able to form in the absence of EzrA. Immunoblotting indicated that FtsZ levels were similar in wild-type and *ezrA* mutant cells throughout the experiment (data not shown).

EzrA Localizes to the Cell Membrane and the Nascent Septal Site. Fractionation of whole-cell extracts from a strain containing an *ezrA-myc* fusion (PL849) indicated that EzrA is tightly associated with the plasma membrane (data not shown). Consistent with this result, live cells expressing a functional *ezrA-gfp* fusion (PL847) had a faint green outline visible around their perimeters (Fig. 2*K*). In addition, in a subset of cells, EzrA was concentrated in a band or ring-like structure at what appeared to be the nascent division site (Fig. 2*K*). In sporulating cells, EzrA-GFP shifted from a medial to a bipolar (or polar) pattern (Fig. 2 *L* and *M*) at approximately the same time as the division site shifts from midcell to polar locations (4). Simultaneous localization of FtsZ-GFP and a fusion of EzrA to a blue variant of GFP (BFP) indicated that the two proteins colocalize to the nascent septal site (Fig. 2 *N–P*).

EzrA Localization Depends on FtsZ. EzrA localization to the nascent septal site, like that of several other cell-division proteins, depended on FtsZ ring formation. To determine the hierarchy of localization, we used a strain (PL851) carrying an EzrA-GFP fusion in which *ftsZ* was under the control of the Lac-repressible IPTG-inducible promoter P$_{spac}$. In cells grown in the presence of IPTG, immunofluorescence microscopy indicated that FtsZ and EzrA-GFP both localized to the

nascent division site (Fig. 2 *Q–S*), consistent with our previous results. However, when cells were examined after four generations of growth in the absence of IPTG, EzrA localization was significantly disrupted. Although there appeared to be an abundance of EzrA-GFP, no EzrA rings were visible in the absence of FtsZ rings (Fig. 2 *T* and *U*). Instead, only a punctate pattern of green fluorescence was observed (Fig. 2*T*). This punctate pattern was apparently caused by fixation methods, because EzrA-GFP was evenly distributed throughout the membrane of live cells grown under the same conditions (data not shown). Preliminary experiments indicate that EzrA localization depends partially on FtsA, another cell-division protein, suggesting that EzrA might not interact directly with FtsZ.

DISCUSSION

During the life of a cell, FtsZ exists in at least two states: monomer and polymer (ring). The transition between these two states, manifested as FtsZ ring assembly and disassembly, is coupled to the cell cycle. Our results are consistent with a model in which EzrA destabilizes the FtsZ polymer, thereby raising the critical concentration of FtsZ required for ring formation (Fig. 4). A null mutation in *ezrA* suppresses the temperature sensitivity of *ftsZ-gfp*, restoring FtsZ ring formation at 45°C. Moreover, the loss of *ezrA* leads to the formation of multiple FtsZ rings in otherwise wild-type cells without altering the concentration of FtsZ. Finally, the critical concentration of FtsZ required for ring formation is lower in *ezrA* null mutants than in wild-type cells.

EzrA, a Negative Regulator of FtsZ Polymerization. The position of the FtsZ ring is governed by the nucleation site, which is postulated to lower the effective concentration of FtsZ required to initiate ring formation (1). *In vivo* FtsZ polymerization is clearly a concentration-dependent phenomenon; decreasing FtsZ levels leads to a cessation of ring formation and eventually cell death (ref. 37; this work). In contrast, overexpression of *ftsZ* leads to the formation of polar FtsZ rings (P.A.L, unpublished data), suggesting that there is a concentration-dependent barrier to FtsZ ring formation at the poles of exponentially growing cells. The efficiency with which polar FtsZ rings form in *ezrA* null mutant cells is consistent with the idea that the critical concentration of FtsZ required for ring formation is lower in the *ezrA* mutants than in wild-type cells, where we propose that EzrA acts to destabilize FtsZ polymers at polar as well as medial sites. Cells encoding two copies of *ezrA* do not exhibit any obvious defects in either cell division or FtsZ localization. For technical reasons, we have not been able to achieve more significant levels of *ezrA* overexpression in *B. subtilis*.
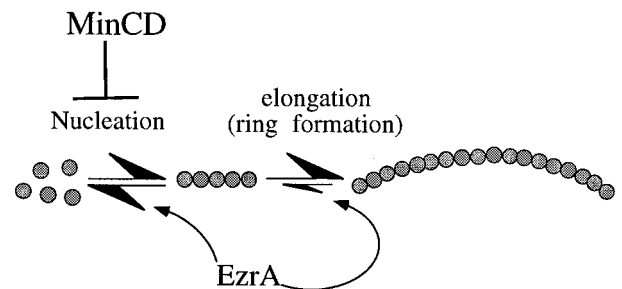
FIG. 4.   Model for FtsZ ring formation. Polymerization is initiated by nucleation of FtsZ monomers forming a short and highly unstable polymer. These short polymers can disassemble rapidly back to monomer or extend to form the longer polymers that constitute the FtsZ ring. In this model, the Min proteins inhibit nucleation of FtsZ, perhaps by competing directly with the monomers for the nucleation sites. EzrA destabilizes already polymerized FtsZ.

Several mechanisms exist by which EzrA could promote destabilization of FtsZ polymers. EzrA may bind directly to the ends of FtsZ polymers and promote rapid depolymerization, a function analogous to that proposed for the kinesin-like protein XKCM1 (38). Alternatively, EzrA could break and/or cap FtsZ polymers in a manner similar to that of the microtubule severing protein Katanin (39). It is also possible that EzrA interacts with other proteins that stabilize the FtsZ ring. In this case, the loss of EzrA might lead to hyperstabilization of the polymers by increasing binding of these stabilizing factors to polymerized FtsZ. Until more is known about FtsZ assembly *in vivo*, it will be difficult to distinguish among these various possibilities.

MinCD vs. EzrA. The distinct localization patterns of *B. subtilis* MinD (11) and EzrA (this work) point to different modes of action. This model is supported by our observation that, in contrast to an *ezrA* null mutation, a null mutation in *minCD* does not suppress the temperature sensitivity of the *ftsZ-gfp* allele. Furthermore, despite the fact that both *ezrA* and *minCD* null mutations result in polar FtsZ rings, the polar sites are used four times more frequently for division in the absence of MinCD than in the absence of EzrA (10).

In light of the polar localization pattern of MinD (11), we postulate that the MinCD complex does not interact directly with FtsZ in *B. subtilis*. Instead, the primary function of the MinCD complex may be to compete with FtsZ for nucleation sites at the cell poles, contributing to the concentration-dependent barrier to FtsZ polymerization at these sites. In contrast, we postulate that EzrA acts throughout the cell, raising the critical concentration of FtsZ required for polymerization at polar and medial sites. At the cell poles, the combined actions of EzrA and MinCD are sufficient to inhibit FtsZ ring formation. The medial nucleation site, however, lowers the barrier to FtsZ polymerization sufficiently to allow ring formation even in the presence of EzrA. Thus, in wild-type cells, we propose that MinCD and EzrA act differently to ensure that FtsZ rings form only at medial division sites.

In summary, we have identified a regulator of FtsZ ring formation, EzrA, which we propose functions similarly to proteins governing microtubule stability in eukaryotic cells. Given the emerging complexity of the bacterial cell cycle, we anticipate that EzrA and MinCD represent just a subset of a class of proteins that modulate FtsZ polymerization, ensuring the precise temporal and spatial regulation of cytokinesis.

1. Lutkenhaus, J. & Addinall, S. G. (1997) *Annu. Rev. Biochem.* **66,** 93–116.
2. Weiss, D. S., Chen, J. C., Ghigo, J. M., Boyd, D. & Beckwith, J. (1999) *J. Bacteriol.* **181,** 508–520.
3. Chen, J. C., Weiss, D. S., Ghigo, J. M. & Beckwith, J. (1999) *J. Bacteriol.* **181,** 521–530.
4. Levin, P. A. & Losick, R. (1996) *Genes Dev.* **10,** 478–488.
5. Mukherjee, A., Cao, C. & Lutkenhaus, J. (1998) *Proc. Natl. Acad. Sci. USA* **95,** 2885–2890.
6. Trusca, D., Scott, S., Thompson, C. & Bramhill, D. (1998) *J. Bacteriol.* **180,** 3946–3953.
7. Hale, C. A. & de Boer, P. A. J. (1997) *Cell* **88,** 175–185.
8. RayChaudhuri, D. (1999) *EMBO J.* **18,** 2372–2383.
9. Rothfield, L. I. & Zhao, C. R. (1996) *Cell* **84,** 183–186.
10. Levin, P. A., Shim, J. J. & Grossman, A. D. (1998) *J. Bacteriol.* **180,** 6048–6051.
11. Marston, A. L., Thomaides, H. B., Edwards, D. H., Sharpe, M. E. & Errington, J. (1998) *Genes Dev.* **12,** 3419–3430.
12. Raskin, D. & de Boer, P. A. J. (1999) *Proc. Natl. Acad. Sci. USA* **96,** 4971–4976.
13. Löwe, J. & Amos, L. A. (1998) *Nature (London)* **391,** 203–206.
14. Nogales, E., Wolf, S. G. & Downing, K. H. (1998) *Nature (London)* **391,** 199–203.
15. Erickson, H. P. (1998) *Trends Cell Biol.* **8,** 133–137.
16. Bramhill, D. & Thompson, C. M. (1994) *Proc. Natl. Acad. Sci. USA* **91,** 5813–5817.
17. Harwood, C. R. & Cutting, S. M. (1990) in *Modern Microbiological Methods*, ed. Goodfellow, M. (Wiley, Chichester, U.K.), p. 569.
18. Sambrook, J., Fritsch, E. F. & Maniatis, T. (1989) *Molecular Cloning: A Laboratory Manual* (Cold Spring Harbor Lab. Press, Plainview, NY).
19. Perego, M., Spiegelman, G. B. & Hoch, J. A. (1988) *Mol. Microbiol.* **2,** 689–699.
20. Jaacks, K. J., Healy, J., Losick, R. & Grossman, A. D. (1989) *J. Bacteriol.* **171,** 4121–4129.
21. Gimeno, R. E., Espenshade, P. & Kaiser, C. A. (1995) *J. Cell Biol.* **131,** 325–338.
22. Lin, D. C.-H., Levin, P. A. & Grossman, A. D. (1997) *Proc. Natl. Acad. Sci. USA* **94,** 4721–4726.
23. Cormack, B. P., Valdivia, R. H. & Falkow, S. (1996) *Gene* **173,** 33–38.
24. Heim, R. & Tsien, R. Y. (1996) *Curr. Biol.* **6,** 178–182.
25. Ireton, K., Rudner, D. Z., Siranosian, K. J. & Grossman, A. D. (1993) *Genes Dev.* **7,** 283–294.
26. Hofmann, K. & Stoffel, W. (1993) *Biol. Chem. Hoppe-Seyler* **347,** 166.
27. Berger, B., Wilson, D. B., Wolf, E., Tonchev, T., Milla, M. & Kim, P. S. (1995) *Proc. Natl. Acad. Sci. USA* **92,** 8259–8263.
28. Harry, E. J., Pogliano, K. & Losick, R. (1995) *J. Bacteriol.* **177,** 3386–3393.
29. Pogliano, K., Harry, E. & Losick, R. (1995) *Mol. Microbiol.* **18,** 459–470.
30. Hiraga, S., Ichinose, C., Niki, H. & Yamazoe, M. (1998) *Mol. Cell* **1,** 381–387.
31. Pogliano, K., Hofmeister, A. E. M. & Losick, R. (1997) *J. Bacteriol.* **179,** 3331–3341.
32. Siemering, K. R., Golbik, R., Sever, R. & Haseloff, J. (1996) *Curr. Biol.* **6,** 1653–1663.
33. Ma, X., Ehrhardt, D. W. & Margolin, W. (1996) *Proc. Natl. Acad. Sci. USA* **93,** 12998–13003.
34. Kunst, F., Ogasawara, N., Moszer, I., Albertini, A. M., Alloni, G., Azevedo, V., Bertero, M. G., Bessieres, P., Bolotin, A., Borchert, S., *et al.* (1997) *Nature (London)* **390,** 249–256.
35. Bi, E. & Lutkenhaus, J. (1993) *J. Bacteriol.* **175,** 1118–1125.
36. Ward, J. E., Jr. & Lutkenhaus, J. (1985) *Cell* **42,** 941–949.
37. Beall, B. & Lutkenhaus, J. (1991) *Genes Dev.* **5,** 447–455.
38. Walczak, C. E., Mitchison, T. J. & Desai, A. (1996) *Cell* **84,** 37–47.
39. McNally, F. J., Okawa, K., Iwamatsu, A. & Vale, R. D. (1996) *J. Cell Sci.* **109,** 561–567.